

## Design, Synthesis, and Conformational Dynamics of a Gated Molecular Basket

Veselin Maslak, Zhiqing Yan, Shijing Xia, Judith Gallucci,  
Christopher M. Hadad, and Jovica D. Badjić\*

Contribution from the Department of Chemistry, The Ohio State University,  
100 West 18th Avenue, Columbus, Ohio 43210

Received January 23, 2006; E-mail: badjić@chemistry.ohio-state.edu

**Abstract:** We have developed a synthesis and examined the conformational behavior and recognition properties of dynamic molecular containers **1–3**. As follows from the  $^1\text{H}$  NMR dilution, diffusion NMR, and vapor pressure osmometry measurements, compound **1** has a low affinity for *intermolecular* aggregation and is mostly present in monomeric form in dilute chloroform solutions. Inspecting the O–H chemical shift resonances of **1**, **3**, and model compound **4** as a function of temperature afforded the  $\Delta\delta/\Delta T$  coefficients of 17.0, 17.3, and 4.7 ppb  $\text{K}^{-1}$ , respectively. In combination with the results from variable temperature  $^1\text{H}$  NMR and IR measurements, the existence of conformers of **1** and **3** in equilibrium, each having a different extent of hydrogen bonding, was confirmed. Molecular mechanics calculations suggested **1<sub>a</sub>** as the most favorable conformation, with three additional conformers, **1<sub>b</sub>**, **1<sub>c</sub>**, and **1<sub>d</sub>**, populating local energy minima. Further optimization of each of the four conformers using semiempirical PM3 and ab initio (HF/6-31G\*) methods allowed a determination of their relative free energies and the corresponding Boltzmann population distributions which were heavily weighted toward **1<sub>a</sub>**. A computed composite IR spectrum of a fraction-weighted mixture of the conformers of **1** reproduced the experimentally observed IR spectrum in its structural features, leading to a conclusion that *conformer 1<sub>a</sub> indeed dominates the equilibrium*. The egg-shaped cavity of **1** (136.6 Å<sup>3</sup>) is complementary in size, shape, and electrostatic potential to chloroform (74.9 Å<sup>3</sup>). A single-crystal X-ray study of **2** revealed a disordered chloroform molecule positioned inside the cavitand along its  $C_3$  axis.

### Introduction

The design and study of molecules that, apart from being receptors, can also regulate kinetics and thermodynamics of the recognition is essential for understanding and linking structure with function in synthetic systems.<sup>1</sup> The inspiration comes from the natural world where traffic of substrates, products, or solutes in and out of the active sites of many enzymes is regulated by the rapid opening and closing of a flaplike “gate” or by conformational adjustments of the macromolecule in response to an external stimulus.<sup>2</sup> Molecular vessels such as cavitands, cyclotrimeratrylenes, carcerands, velcrands, trinacrenes, self-

assembled capsules, and metal-assembled cage molecules have been constructed to surround a target molecule and selectively recognize it.<sup>3</sup> Housing a guest in this manner allowed its protection from external reactants<sup>4</sup> and transport between phases<sup>5</sup> and provided a molecular reaction domain.<sup>6</sup> The controlled release of small molecules by hemicarceplexes, metal-containing self-assembled molecular cages, or self-assembled capsules has

- (1) (a) Mogck, O.; Pons, M.; Boehmer, V.; Vogt, W. *J. Am. Chem. Soc.* **1997**, *119*, 5706–5712. (b) Vysotsky, M. O.; Thondorf, I.; Bohmer, V. *Angew. Chem., Int. Ed.* **2000**, *39*, 1264–1267. (c) Davis, A. V.; Yeh, R. M.; Raymond, K. N. *Proc. Natl. Acad. Sci. U.S.A.* **2002**, *99*, 4793–4796. (d) Zhong, Z.; Anslyn, E. V. *Angew. Chem., Int. Ed.* **2003**, *42*, 3005–3008. (e) Davis, J. T.; Kaucher, M. S.; Kotch, F. W.; Iezzi, M. A.; Clover, B. C.; Mullaugh, K. M. *Org. Lett.* **2004**, *6*, 4265–4268. (f) Heemstra, J. M.; Moore, J. S. *J. Org. Chem.* **2004**, *69*, 9234–9237. (g) Gianneschi, N. C.; Cho, S.-H.; Nguyen, S. B. T.; Mirkin, C. A. *Angew. Chem., Int. Ed.* **2004**, *43*, 5503–5507. (h) Zuccaccia, D.; Pirondini, L.; Pinalli, R.; Dalcanele, E.; Macchioni, A. *J. Am. Chem. Soc.* **2005**, *127*, 7025–7032. (i) Rebek, J., Jr. *Angew. Chem., Int. Ed.* **2005**, *44*, 2068–2078.
- (2) (a) Nolte, H.-J.; Rosenberry, T. L.; Neumann, E. *Biochemistry* **1980**, *19*, 3705. (b) McCammon, J. A.; Northrup, S. H. *Nature* **1981**, *293*, 316. (c) Sussman, J. L.; Harel, M.; Frolow, F.; Oefner, C.; Goldman, A.; Tokor, L.; Silman, I. *Science* **1991**, *253*, 872–879. (d) Wlodek, S. T.; Clark, T. W.; Scott, L. R.; McCammon, J. A. *J. Am. Chem. Soc.* **1997**, *119*, 9513–9522. (e) Zhou, H.-X.; Wlodek, S. T.; McCammon, J. A. *Proc. Natl. Acad. Sci.* **1998**, *95*, 9280.

- (3) (a) Moran, J. R.; Karbach, S.; Cram, D. J. *J. Am. Chem. Soc.* **1982**, *104*, 5826–5828. (b) Moran, J. R.; Ericson, J. L.; Delcanale, E.; Bryant, J. A.; Knobler, C. B.; Cram, D. J. *J. Am. Chem. Soc.* **1991**, *113*, 5707–5714. (c) Ashton, P. R.; Girreser, U.; Giuffrida, D.; Kohnke, F. H.; Mathias, J. P.; Raymo, F. M.; Slawin, A. M. Z.; Stoddart, J. F. *J. Am. Chem. Soc.* **1993**, *115*, 5422–5429. (d) Collet, A.; Dataset, J. P.; Lozach, B.; Canceill, J. *Top. Curr. Chem.* **1993**, *165*, 103–129. (e) Ikeda, A.; Shinkai, S. *Chem. Rev.* **1997**, *97*, 1713–1734. (f) Jasat, A.; Sherman, J. C. *Chem. Rev.* **1999**, *99*, 931–967. (g) Caulder, D. L.; Raymond, K. N. *Acc. Chem. Res.* **1999**, *32*, 975–982. (h) Tucci, F.; Rudkevich, D. M.; Rebek, J., Jr. *Chem.—Eur. J.* **2000**, *6*, 1007–1016. (i) Fox, O. D.; Drew, M. G. B.; Beer, P. D. *Angew. Chem., Int. Ed.* **2000**, *39*, 136–140. (j) Hof, F.; Craig, S. L.; Nuckolls, C.; Rebek, J., Jr. *Angew. Chem., Int. Ed.* **2002**, *41*, 1488–1508. (k) Sun, W. J.; Yoshizawa, M.; Kusukawa, T.; Fujita, M. *Curr. Opin. Chem. Biol.* **2002**, *6*, 757–764. (l) Kryschenko, Y. K.; Seidel, S. R.; Arif, A. M.; Stang, P. J. *J. Am. Chem. Soc.* **2003**, *125*, 5193–5198. (m) Casnati, A.; Sansone, F.; Ungaro, R. *Acc. Chem. Res.* **2003**, *36*, 246–254. (n) Ryu, E.-H.; Zhao, Y. *Org. Lett.* **2004**, *6*, 3187–3189. (o) Van, L.; Fijs, W. B.; Beijleveld, H.; Kooijman, H.; Spek, A. L.; Verboom, W.; Reinhoudt, D. N. *J. Org. Chem.* **2004**, *69*, 3928–3936. (p) Dalgarno, S. J.; Tucker, S. A.; Bassil, D. B.; Atwood, J. L. *Science* **2005**, *309*, 2037–2039. (q) Isaacs, L.; Park, S.-K.; Liu, S.; Ko, Y. H.; Selvapalam, N.; Kim, Y.; Kim, H.; Zavalij, P. Y.; Kim, G.-H.; Lee, H.-S.; Kim, K. *J. Am. Chem. Soc.* **2005**, *127*, 18000–18001. (r) Rudkevich, D. M.; Kang, Y.; Leontiev, A. V.; Organo, V. G.; Zyryanov, G. V. *Supramol. Chem.* **2005**, *17*, 93–99. (s) Azov, V. A.; Schlegel, A.; Diederich, F. *Angew. Chem., Int. Ed.* **2005**, *44*, 4635–4638.

been investigated.<sup>7</sup> However, the regulation of the kinetics of molecular recognition, i.e., guest transport in/out of the host, in synthetic receptors is still a challenging task. Rebek et al. have recently recognized<sup>8</sup> that the energy barrier for guest exchange in resorcinarene-based cavitands can be controlled by restricting their conformational dynamics. A set of amide groups installed at the rim of the resorcinarene led to the formation of a net of hydrogen bonds at the cavity opening that rigidified the cavitand's conformation. Remarkably, upon accommodating a target guest molecule, these cavitands formed complexes with high kinetic stabilities despite their open-ended structures and low binding affinities. It is plausible that gaining control over the kinetics of in/out molecular shuttling for artificial receptors will allow the following: (a) regulation of useful and encapsulated reaction chemistry, (b) development of novel and efficient molecular devices for delivery purposes, and (c) direct engineering of controllable ion and molecular channels. In that perspective, our efforts are focused on the design of molecular containers having a set of *stimuli-responsive gates*, to enclose space and thus regulate the incarceration of target molecules, as depicted in Figure 1. In the study described here, we report on the synthesis, conformational analysis, and preliminary recognition properties of molecular containers 1–3 (Figure 1). These compounds have a flat aromatic base which is fused to three bicyclo[2.2.1]heptane rings to form a curved unit. Three phthalimides extend this curvature into a rigid bowl-shaped cavitand, to which three aromatic gates, each containing a single CH<sub>2</sub> rotor and, in 1 and 3, a pH responsive OH group, are appended. We envision that (a) these three aromatics will assemble on top of the cavitand, by way of directed intramolecular O–H···O hydrogen bonds, and thereby serve as gates to regulate in/out exchange of guests and (b) the rate of opening and closing of the gates, and therefore the kinetics of the guest exchange, will be controlled by pH to regulate their degree of protonation. Phenolic host molecules such as hydroquinone,

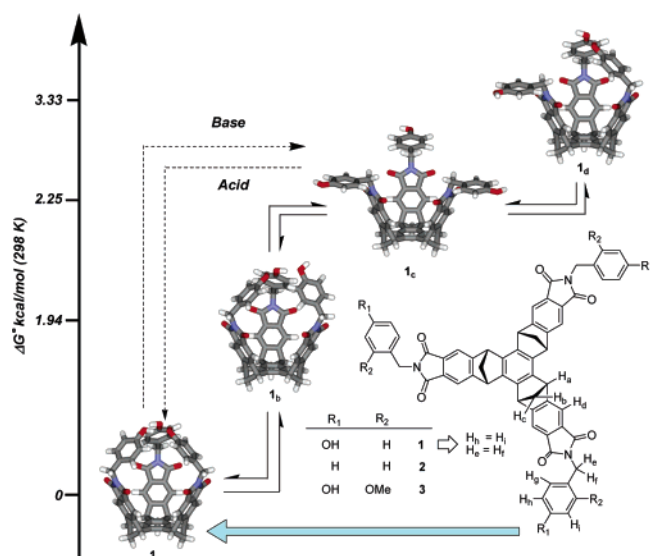


**Figure 1.** Energy minimized (Hartee-Fock, HF/6-31G\*) conformations **1a**, **1b**, **1c**, and **1d** and their calculated relative standard free energies  $\Delta G^\circ$ ; based on the calculation, the conformer **1a** dominates the equilibrium state, 94%. Chemical structures of dynamic receptors **1–3**, with their <sup>1</sup>H NMR spectroscopic assignment. An external base/acid input is envisioned to drive the opening and closing of **1** (see Figure 6).

phenol, and Dianin's compound are known to form hydrogen-bonded clathrates containing hexameric units of hosts stacked on top of each other to encapsulate guests between the sextets.<sup>9</sup> Integrated into dynamic receptors, but only in a multivalent fashion, phenols are herein designed to assemble in a comparable manner.

The design and study of **1–3** as gated molecular baskets as well as their related analogues are directed at expanding our fundamental knowledge of noncovalent forces which can drive molecular self-assembly and at developing the important principles for creating dynamic receptors. Moreover, elucidating the mechanism by which these dynamic hosts operate will aid in the predictable incorporation of their dynamic behavior toward building more efficient receptors for various applications.

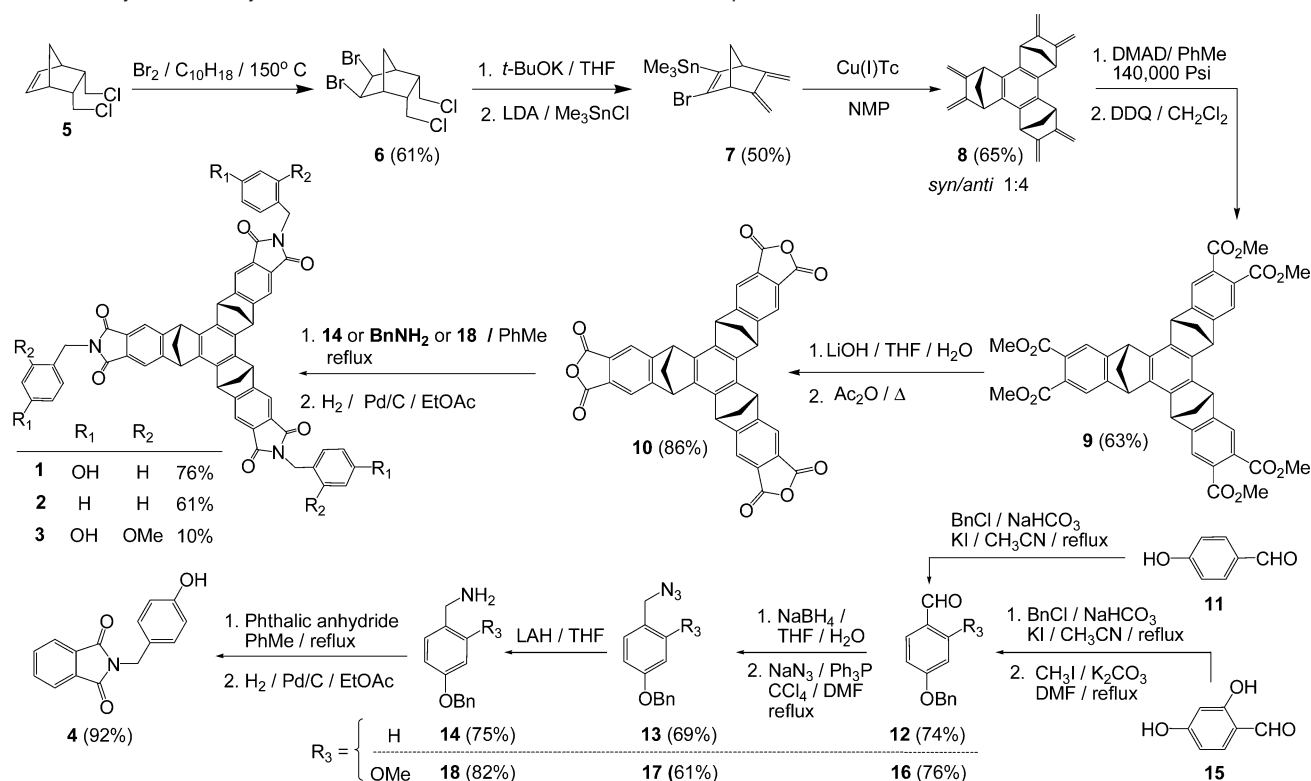
## Results and Discussion

**Synthesis.** The synthesis of **1–3** is outlined in Scheme 1. The originally reported methodology for the preparation of **8** has been modified by us.<sup>10</sup> Diels–Alder cycloaddition of cyclopentadiene to *cis*-1,4-dichloro-2-butene, in refluxing benzene, gave compound **5** in 71% yield. The bromination of **5** to yield **6** was entailed with some difficulties.

We noticed that the reaction temperature had a dramatic effect on the product distribution. At room temperature, the reaction gave the products of Wagner–Meerwein rearrangement, which could be rationalized by an ionic addition of Br<sub>2</sub> to norbornene mediated by a  $\sigma$ -bridged nonclassical 2-norbornyl cation intermediate.<sup>11</sup> In boiling decalin at 150 °C, the addition of bromine to **5** was not accompanied with significant skeletal rearrangements and yielded **6** as the major product, through, as

- (4) (a) Cram, D. J.; Tanner, M. E.; Thomas, R. *Angew. Chem., Int. Ed. Engl.* **1991**, *30*, 1024–1027. (b) Kurdستاني, S. K.; Helgeson, R. C.; Cram, D. J. *J. Am. Chem. Soc.* **1995**, *117*, 1659–1960. (c) Warmuth, R.; Marvel, M. A. *Angew. Chem., Int. Ed.* **2000**, *39*, 1117–1119. (d) Marquez, C.; Nau, W. M. *Angew. Chem., Int. Ed.* **2001**, *40*, 4387–4390. (e) Ziegler, M.; Brumaghim, J. L.; Raymond, K. N. *Angew. Chem., Int. Ed.* **2000**, *39*, 4119–4121. (f) Makeiff, D. A.; Vishnumurthy, K.; Sherman, J. C. *J. Am. Chem. Soc.* **2003**, *125*, 9558–9559. (g) Kaanumalle, L. S.; Gibb, C. L. D.; Gibb, B. C.; Ramamurthy, V. *J. Am. Chem. Soc.* **2004**, *126*, 14366–14367. (h) Kirmse, W. *Angew. Chem., Int. Ed.* **2005**, *44*, 2476–2479. (i) Hooley, R. J.; Rebek, J., Jr. *J. Am. Chem. Soc.* **2005**, *127*, 11904–11905. (5) Rudkevich, D. M. *Bull. Chem. Soc. Jpn.* **2002**, *75*, 393–413. (6) (a) Beno, B. R.; Sheu, C.; Houk, K. N.; Warmuth, R.; Cram, D. J. *Chem. Commun.* **1998**, *3*, 301–302. (b) Yoshizawa, M.; Takeyama, Y.; Kusukawa, T.; Fujita, M. *Angew. Chem., Int. Ed.* **2002**, *41*, 1347–1349. (c) Fiedler, D.; Bergman, R. G.; Raymond, K. N. *Angew. Chem., Int. Ed.* **2004**, *43*, 6748–6751. (d) Vriezema, D. M.; Aragonés, M. C.; Elemans, J. A. A.; Cornelissen, J. J. L. M.; Rowan, A. E.; Nolte, R. J. M. *Chem. Rev.* **2005**, *105*, 1445–1489. (e) Purse, B. W.; Rebek, J., Jr. *Proc. Natl. Acad. Sci. U.S.A.* **2005**, *102*, 10777–10782. (f) Purse, B. W.; Gissot, A.; Rebek, J., Jr. *J. Am. Chem. Soc.* **2005**, *127*, 11222–11223. (g) Cacciapaglia, R.; Casnati, A.; Mandolini, L.; Reinhoudt, D. N.; Salvio, R.; Sartori, A.; Ungaro, R. *J. Org. Chem.* **2005**, *70*, 5398–5402. (7) (a) Robbins, T. A.; Cram, D. J. *J. Chem. Soc., Chem. Commun.* **1995**, *15*, 1515–1516. (b) Sherman, J. C. *Tetrahedron* **1995**, *51*, 3395–422. (c) Branda, N.; Grotzfeld, R. M.; Valdes, C.; Rebek, J., Jr. *J. Am. Chem. Soc.* **1995**, *117*, 85–88. (d) Houk, K. N.; Nakamura, K.; Sheu, C.; Keating, A. E. *Science* **1996**, *273*, 627–629. (e) Piatnitski, E. L.; Deshayes, K. D. *Angew. Chem., Int. Ed.* **1998**, *37*, 970–973. (f) Place, D.; Brown, J.; Deshayes, K. D. *Tetrahedron Lett.* **1998**, *39*, 5915–5918. (g) Kerckhoffs, J. M. C. A.; van Leeuwen, F. W. B.; Spek, A. L.; Kooijman, K.; Crego-Calama, M.; Reinhoudt, D. N. *Angew. Chem., Int. Ed.* **2003**, *42*, 5717–5722. (h) Hiraoka, S.; Harano, K.; Shiro, M.; Shionoya, M. *Angew. Chem., Int. Ed.* **2005**, *44*, 2727–2731. (i) Davis, A. V.; Raymond, K. N. *J. Am. Chem. Soc.* **2005**, *127*, 7912–7919. (8) (a) Rudkevich, D. M.; Hilmersson, G.; Rebek, J., Jr. *J. Am. Chem. Soc.* **1997**, *119*, 9911–9912. (b) Rudkevich, D. M.; Hilmersson, G.; Rebek, J., Jr. *J. Am. Chem. Soc.* **1998**, *120*, 12216–12225.

- (9) Atwood, J. L.; Davies, J. E. D.; MacNicol, D. D., Eds. *Inclusion Compounds*; Academic Press: London, U.K., 1984; Vol 2. (10) Borsato, G.; De Lucchi, O.; Fabris, F.; Lucchini, V.; Pasqualotti, M.; Zambon, A. *Tetrahedron Lett.* **2002**, *44*, 561–563. (11) (a) Colter, A.; Friedrich, E. C.; Holness, N. J.; Winstein, S. *J. Am. Chem. Soc.* **1965**, *87*, 378–379. (b) Walling, C. *Acc. Chem. Res.* **1983**, *16*, 448–454.

**Scheme 1.** Synthesis of Dynamic Molecular Containers 1–3 and Model Compound 4

we believe, a radical process.<sup>12</sup> The preferred stereochemistry of the *cis* addition, occurring from the *exo* side, has been confirmed by 2D-NOESY measurements. The compound **6**, upon successive halogen eliminations using *t*-BuOK and then stanannylation, afforded the bromo(trimethylstannyl)triene **7**. Cyclootrimerization of **7**, promoted by copper(I) thiophenylcarboxylate (Cu(I)Tc), yielded **8** as a 4:1 mixture of *anti* and *syn* isomers in 65% isolated yield. The desired *syn* isomer was successfully separated from the *anti* using column chromatography. We initially anticipated that **8** would be highly reactive in Diels–Alder reactions.<sup>10</sup> Interestingly, the cycloaddition of a reactive dienophile, dimethyl acetylenedicarboxylate (DMAD), to **8** had to be performed at a high pressure in order to yield **9**, after the DDQ aromatization step. Hexaester **9** was then converted to a stable tris-anhydride **10**, which, in a reaction with **14**, benzylamine, or **18**, followed by subsequent hydrogenolysis, yielded **1**, **2**, and **3**, in 76, 61, and 10% yield, respectively. For the preparation of **14**, commercially available 4-hydroxybenzaldehyde **11** was converted to **13** that in a reaction with LiAlH<sub>4</sub> yielded **14** as a major product. Similarly, 4-benzyloxy-2-methoxybenzylamine **18** was synthesized starting from 2,4-dihydroxybenzaldehyde **15**. The model compound **4** was obtained by reacting phthalanhydride with 4-benzyloxybenzylamine **14**, followed by hydrogenolysis promoted with Pd/C catalyst.

**Solubility and Sample Preparation.** The solubility of **1** and **3** was very low in a range of neat organic solvents. We discovered that the addition of methanol to a suspension of **1** or **3** in chloroform afforded a homogeneous solution. The evaporation of such a prepared solution to dryness, using elevated temperature in vacuo, afforded the desired compound

which was then readily soluble in chloroform or dichloromethane. This observation provided qualitative evidence that both of these two solvents efficiently solvate the interior of **1** and **3**, and as such, render them soluble. It is likely that methanol, as a polar hydrogen bonding solvent, aided the solvation process by breaking the crystal lattice of **1** and **3**. Interestingly, **2** was directly solubilized in nonpolar organic solvents, without any pretreatment of its solutions with methanol.

**<sup>1</sup>H NMR Spectroscopic Studies.** Compounds **1–3** were characterized by <sup>1</sup>H NMR spectroscopy, including <sup>1</sup>H–<sup>1</sup>H COSY and TROESY two-dimensional experiments in order to achieve full structural assignment. The <sup>1</sup>H NMR spectrum of **1** in dry CDCl<sub>3</sub> is assigned to a molecule with averaged C<sub>3v</sub> symmetry, Figure 2a. The signal for its O–H proton shifted upfield (from 6.88 to 6.66 ppm) as the CDCl<sub>3</sub> solution was diluted (from 3.8 to 0.5 mM) and then stayed constant after further dilution. The <sup>1</sup>H NMR signal for the O–H proton of the model compound **4** (Figure 2b) also shifted to higher field, from 4.79 to 4.63 ppm with 30.0 to 1.0 mM dilution, and then stayed constant at lower concentrations. The observed dependence of the O–H resonance shift with the concentration of both **1** and **4** provides some evidence for *intermolecular* hydrogen-bonding interactions which decreased upon dilution. The small magnitude of the shift, however, signified nonextensive aggregation.

The model compound **4** self-associates via intermolecular hydrogen bonding. Assuming a linear aggregation of **4** in solution, the nonlinear curve fitting of its dilution <sup>1</sup>H NMR data to an EK isodesmic mathematical model yielded an apparent association constant of 53 ± 10 M<sup>-1</sup>.<sup>13</sup> From this analysis, the normalized weight fraction for the oligomeric distribution

(12) Tutar, A.; Taskesenligil, Y.; Cakmak, O.; Abbasoglu, R.; Balci, M. *J. Org. Chem.* **1996**, *61*, 8297–8300.

(13) Martin, R. B. *Chem. Rev.* **1996**, *96*, 3943–3063.

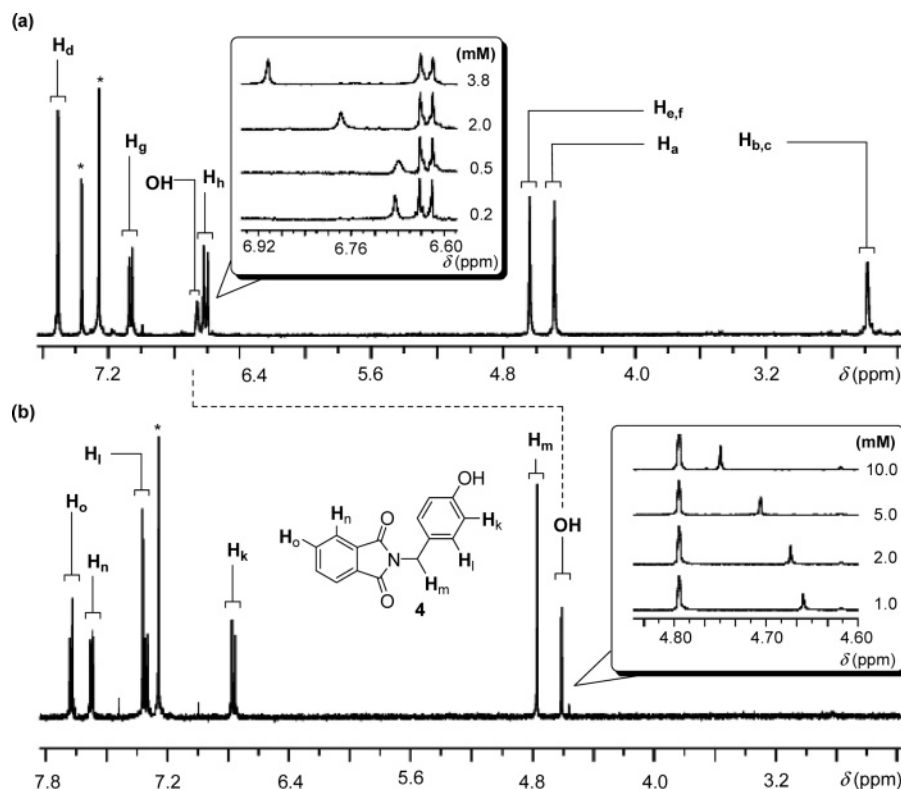


**Figure 2.**  $^1\text{H}$  NMR spectra (400 MHz, 298 K) of (a) **1** (0.5 mM) and (b) **4** (1.0 mM), in dry  $\text{CDCl}_3$ . Insets: segments of  $^1\text{H}$  NMR spectra, showing the O–H resonance shifts of **1** (top) and **4** (bottom) obtained in dilution experiments.

indicates that 82% of the nonassociated and 15% of dimeric **4** are present in the 5.0 mM solution. A low propensity of **4** for having intermolecular association is particularly evident. The trivalent **1**, however, could form both inter- and intramolecular hydrogen bonds. A nearly complete absence of *intermolecular* association or aggregation is suggested by the invariant O–H chemical shift observed in 0.5 mM or less concentrated solutions of **1** (see inset in Figure 2a).

**Vapor Pressure Osmometry.** The intermolecular association of **1** and **4** was also examined using vapor pressure osmometry (VPO). It is important to note that, in this technique, the experimental molecular weight of the unknown is a weighted average of the molecular weights of its free and aggregated molecules.<sup>14</sup> Calibration with a standard is required, and consequently, the results are dependent on the choice of the standard.<sup>15</sup> The observed molecular weight of the model **4** (calculated  $M_w = 253$ ) varied between  $256 \pm 5$  and  $325 \pm 7$  for its 3.7–8.3 mM chloroform solutions, Figure 3a. A low degree of intermolecular aggregation over this concentration range is evident, and these results are in accord with the  $^1\text{H}$  NMR chemical shifts and spectra. The VPO measurements of **1**, using sucrose octaacetate and triacetyl- $\beta$ -cyclodextrin as standards, showed that the observed molecular weight deviates, but not drastically, about the value calculated for the free **1** ( $M_w = 946$ ), Figure 3b. At lower concentrations, the observed molecular weights were below (almost 48%!) the expected value and is presumably a result of the large experimental uncertainty at those concentrations. The difference in the voltage ( $\Delta V$ )

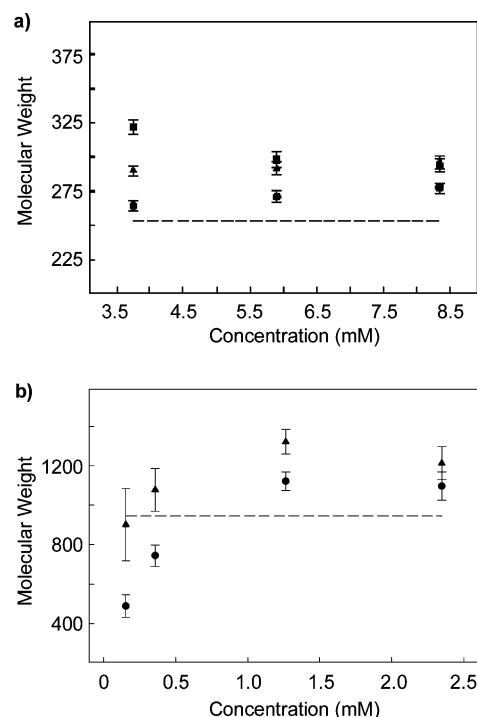


**Figure 3.** Vapor pressure osmometry determined molecular weights of (a) model compound **4** and (b) dynamic receptor **1**, in dry chloroform at 310 K, using sucrose octaacetate ( $\bullet$ ), triacetyl- $\beta$ -cyclodextrine ( $\blacktriangle$ ), and benzil ( $\blacksquare$ ) as standards. The error bars correspond to the standard deviations of the VPO measurements of the sample.

between the thermister beads in the osmometer is proportional to the difference in the vapor pressures of the solvent and the sample. The voltage change is smaller when the concentration of the sample ( $C$ ) is decreased so the measured  $\Delta V/C$ , used to

(14) (a) Solie, T. N. *Methods Enzymol.* **1972**, *26*, 50. (b) Hiroki, S.; Takahira, Y.; Yamaguchi, M. *J. Org. Chem.* **2005**, *70*, 5698–5708.

(15) Seto, C. T.; Whitesides, G. M. *J. Am. Chem. Soc.* **1993**, *115*, 905–916. (b) Zimmerman, S. C.; Zeng, F.; Reichert, D. E. C.; Kolotuchin, S. V. *Science* **1996**, *271*, 1095–98.

determine the molecular weight, becomes uncertain in highly dilute solutions. Nonetheless, these experiments unambiguously suggested that, in the examined range of chloroform concentrations, **1** is mostly present in its monomeric state.

**Diffusion NMR Spectroscopy.** HR-DOSY<sup>16</sup> measurements additionally confirmed the low propensity of **1** for intermolecular association. The observed diffusion coefficient of **1**, in its 0.3–1.0 mM CDCl<sub>3</sub> solutions, increased from  $5.50 \times 10^{-10}$  to  $6.17 \times 10^{-10}$  m<sup>2</sup> s<sup>-1</sup>. Importantly, under the conditions of fast chemical exchange, the observed diffusion coefficient  $D$  of the unknown has the average value of the free  $D_{\text{free}}$  and bound  $D_{\text{bound}}$  states weighted by their fraction.<sup>17</sup> The slight variation in the experimentally determined diffusion coefficients with concentration, therefore, indicated insignificant alternations in the equilibrium composition and, all together with the <sup>1</sup>H NMR dilution and VPO studies, confirmed that **1** is indeed “free” in dilute chloroform solutions.

**Conformational Studies. <sup>1</sup>H NMR Spectroscopy.** Ruling out the aggregation of **1** allowed us to investigate its conformational behavior. The resonance shift for the O–H groups in the <sup>1</sup>H NMR spectrum of **1** is positioned downfield with respect to the O–H signal for the model compound **4**,  $\Delta\delta = 2.03$  ppm (see Figure 2). It is reasonable to ascribe this observation to the existence of *intramolecular* hydrogen-bonding interactions involving the three phenol gates of the capsule. Recall that the <sup>1</sup>H NMR spectrum of **1** is assigned to a molecule with averaged  $C_{3v}$  symmetry, and this indicates (a) the simultaneous presence of different conformers of **1** in rapid exchange on the NMR time scale or (b) the exclusive presence of a  $C_{3v}$  symmetrical conformer (as shown in Figure 1). To examine these possibilities, variable temperature <sup>1</sup>H NMR spectra were recorded for the dynamic containers **1** and **3** and the model compound **4** in CDCl<sub>3</sub>. In the case of **1** and **3**, as the CDCl<sub>3</sub> solution was cooled from 323 to 223 K, notable changes in the chemical shifts and broadening of the signals for the H<sub>g</sub>, H<sub>h</sub>, and H<sub>i</sub> protons as well as H<sub>e,f</sub> were observed (see Figure 1 for the hydrogen assignments), while the signals for the other protons were unaffected. Furthermore, the appearance of new resonances, or the coalescence of existing ones, did not occur for **1** and **3**. In the case of the model compound **4**, however, no changes were observed when its CDCl<sub>3</sub> solution was cooled across the same temperature range. Since the protons of the aromatic gates, present in both **1** and **3**, experienced chemical shift and line broadening at lower temperatures, the spectral results are commensurate with a change in the conformational distribution of the aryl gate that is occurring rapidly on the NMR time scale. Inspecting the O–H resonance shifts of **1**, **3**, and **4** with temperature allowed us to calculate the corresponding temperature-dependent, chemical-shift coefficients  $\Delta\delta/\Delta T$  for the 223 to 323 K interval as shown in Figure 4. The magnitude of this value provides qualitative information about the structure of the molecule of interest.<sup>18</sup> Namely, as the hydroxyl proton is rapidly exchanging among its hydrogen-bonded and non-hydrogen-bonded conformations, the observed chemical-shift signal represents a weighted average of the signals for the same proton in its alternative environments;

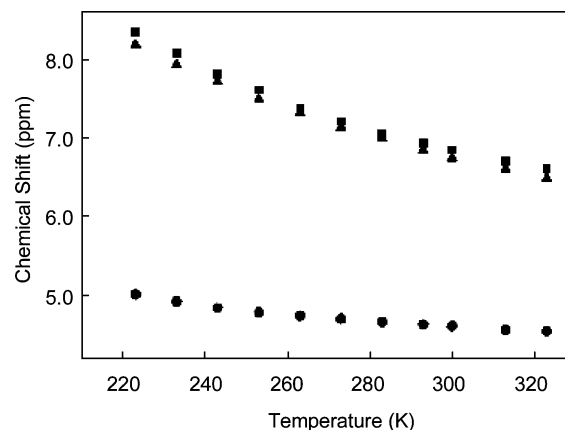


**Figure 4.** <sup>1</sup>H NMR chemical shifts for the O–H in **1** (▲, 0.5 mM), **3** (■, 0.5 mM), and **4** (●, 1.0 mM) in dry CDCl<sub>3</sub> as a function of temperature. Based on these data, temperature dependence chemical shift coefficients  $\Delta\delta/\Delta T$ , 223–323 K, were calculated to be  $17.0 \times 10^{-3}$  ppm K<sup>-1</sup> for **1**,  $17.3 \times 10^{-3}$  ppm K<sup>-1</sup> for **3**, and  $4.7 \times 10^{-3}$  ppm K<sup>-1</sup> for **4**.

that is, the higher the chemical shift, the more extensive the hydrogen-bonding becomes. A small, but positive, temperature coefficient ( $4.7 \times 10^{-3}$  ppm K<sup>-1</sup>) is calculated for **4** and implies a somewhat intensified hydrogen-bonding interaction as the temperature is lowered (Figure 4). Evidently, the model compound aggregates to a small extent at lower temperatures. In contrast, the temperature coefficient calculated for the O–H resonance in **1** and **3** ( $17.0 \times 10^{-3}$  and  $17.3 \times 10^{-3}$  ppm K<sup>-1</sup>, respectively) was significantly bigger. The existence of the conformers of **1** and **3** in equilibrium, each having a different extent of hydrogen bonding, could account for this result, as the corresponding equilibrium constant is likely to be quite receptive to a temperature change. To a first approximation, extensive intermolecular aggregation of **1** at low temperatures can be eliminated when compared to the behavior of model compound **4**.

**Infrared Spectroscopy and Theoretical Calculations.** The conformational behavior of **1** and **4** was also thoroughly examined using infrared spectroscopy in combination with theoretical calculations. First, let us analyze the model compound **4**. As shown in Figure 5a, the FT-IR spectra of 0.4 to 4.8 mM CHCl<sub>3</sub> solutions of the model compound **4** revealed two O–H stretching vibrations, one strong at 3597 cm<sup>-1</sup> and one weak at 3466 cm<sup>-1</sup>, corresponding to free and hydrogen-bonded O–H groups, respectively. HF/6-31G\* calculations<sup>19</sup> of the optimized geometries and the resultant harmonic vibrational frequencies of monomeric and dimeric forms of **4** confirmed this assignment (Figure 5c). Moreover, the experimental spectrum was simulated by a curve-fitting routine (IGOR<sup>20</sup>) using two Gaussian functions centered at the calculated peak positions. In this simulation, the broadening (fwhm) of each peak was kept the same for both calculated peaks so as to simulate the experimental spectrum of the monomeric and dimeric **4**. The resulting simulated IR spectrum clearly reproduced the features of its experimentally recorded spectrum, and from this analysis, we determined that the 4.8 mM CHCl<sub>3</sub> spectrum of **4** was composed of the monomeric (89%) and dimeric (11%) forms. Furthermore, this

(16) Cohen, Y.; Avram, L.; Frish, L. *Angew. Chem., Int. Ed.* **2005**, *44*, 520–554.

(17) Cabrita, E. J.; Berger, S. *Magn. Reson. Chem.* **2002**, *40*, S122–127.

(18) For instance, see: (a) Gellman, S. H.; Adams, B. R.; Dado, G. P. *J. Am. Chem. Soc.* **1990**, *112*, 460–461. (b) Winningham, M. J.; Sogah, D.; Sogah, D. Y. *J. Am. Chem. Soc.* **1994**, *116*, 11173–11174.

(19) (a) Hehre, W. J.; Radom, L.; Schleyer, P. v. R.; Pople, J. A. *Ab initio Molecular Orbital Theory*; John Wiley & Sons: New York, 1986. (b) Frisch, M. J. et al. *Gaussian 03*, revision C.02; Gaussian, Inc.: Wallingford, CT, 2004.

(20) 1988–2004 WaveMetrics, Inc. version: 5.0.2.0. More information can be found at <http://www.wavemetrics.com>.

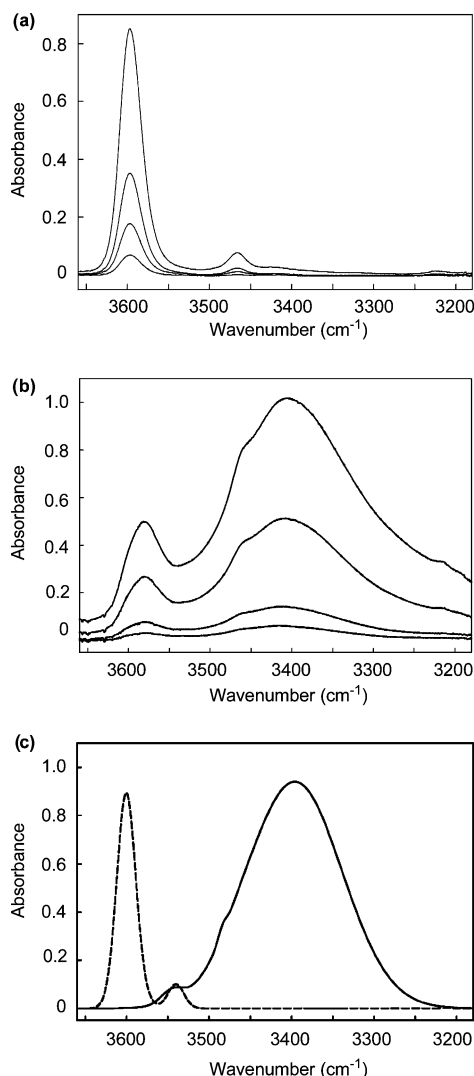


**Figure 5.** O–H stretch region of infrared spectra for (a) 4.8, 2.0, 1.0, and 0.4 mM  $\text{CHCl}_3$  solution of **4** and (b) 4.4, 2.1, 0.6, and 0.2 mM  $\text{CHCl}_3$  solution of **1**. The spectra were obtained after subtraction of the spectrum of pure  $\text{CHCl}_3$ . (c) Calculated IR spectrum (Hartree–Fock, HF/6-31G\*) of a fraction-weighted mixture of free and dimeric **4** (dashed line). Calculated IR spectrum of a fraction-weighted mixture of the conformers of **1** (solid line). The standard free energies for each conformer of **1** were calculated using Hartree–Fock theoretical method (HF/6-31G\*). Vibrational frequencies were calculated using the semiempirical PM3 theoretical method. Note that the simulated spectra are deliberately shifted,  $160\text{ cm}^{-1}$  for **4** and  $245\text{ cm}^{-1}$  for **1**, to visually overlap the experimentally obtained results.

analysis indicated a low degree of intermolecular association which is in accord with the prior experiments.

The FT-IR spectra of 0.2 to 4.4 mM  $\text{CHCl}_3$  solutions of **1** revealed three concentration-invariant O–H stretching vibrations, two strong and broad bands at  $3581$  and  $3402\text{ cm}^{-1}$  and a shoulder at  $3460\text{ cm}^{-1}$  (Figure 5b). The signal at  $3581\text{ cm}^{-1}$  in **1** is at a slightly lower wavenumber than the free O–H stretching vibration at  $3697\text{ cm}^{-1}$  in the model compound **4**. The signal at  $3402\text{ cm}^{-1}$ , however, may well be due to intramolecularly associated O–H groups. In parallel with the  $^1\text{H}$  NMR spectroscopic measurements, these results point to the existence of a conformational equilibrium in **1**. Which conformers then populate the equilibrium state of **1**? As implemented in MacroModel,<sup>21</sup> the results of molecular mechanics (MMFF) calculations suggested **1<sub>a</sub>** as the most favorable conformation, and with three additional conformers, **1<sub>b</sub>**, **1<sub>c</sub>**, and **1<sub>d</sub>**, populating

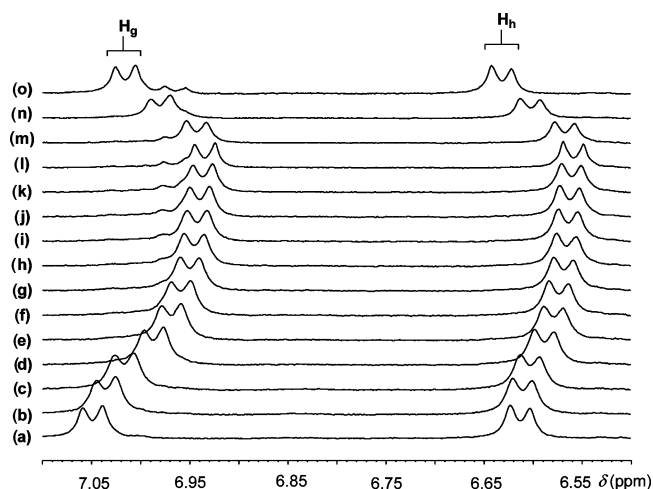


**Figure 6.** A series of partial  $^1\text{H}$  NMR spectra of **1** (400 MHz, 298 K) recorded on addition of  $\text{Et}_3\text{N}$  (a–l) and  $\text{CF}_3\text{CO}_2\text{H}$  (m–o) to a 1.0 mM  $\text{CDCl}_3$  solution; (a) 0, (b) 0.24, (c) 0.48, (d) 0.96, (e) 1.44, (f) 1.92, (g) 2.64, (h) 3.36, (i) 4.32, (j) 5.52, (k) 7.92, (l) 9.12 mol equiv of  $\text{Et}_3\text{N}$ , and (m) 3.90, (n) 7.80, (o) 11.70 mol equiv of  $\text{CF}_3\text{CO}_2\text{H}$ .

local energy minima, as shown in Figure 1. Predicting the hydrogen-bonded mediated folding pattern of small molecules with molecular mechanics is indeed debatable and has already been addressed in parametrizing various force fields.<sup>22</sup> Therefore, we further optimized each of the four conformers using both semiempirical PM3<sup>23</sup> and ab initio Hartree–Fock (HF/6-31G\*) methods<sup>19</sup> to (1) calculate their relative free energies, (2) estimate their Boltzmann population distribution, and (3) calculate harmonic vibrational frequencies so as to simulate their composite infrared spectra. Based on the free energies (Figure 1), conformer **1<sub>a</sub>** having all three phenols involved in a cyclic array of the intramolecular hydrogen bonding is the most stable and largely populates the equilibrium, 94%. Conformer **1<sub>b</sub>**, having three phenols interacting intramolecularly but forming a linear array of only two hydrogen bonds, is less stable and populates 3.5% of the equilibrium. The partially open **1<sub>d</sub>** (one H-bond) and fully open **1<sub>c</sub>** (no H-bonds) conformers are energetically unfavored and contribute only 2.5% to the equilibrium. With this information in hand, we computed a composite IR spectrum of a fraction-weighted mixture of the conformers of **1**, using computer-generated Gaussian-broadened functions for each O–H vibrational frequency for each conformer, Figure 5c. The simulated spectrum of **1** does indeed reproduce the experimental spectrum in its features. All three IR bands are visible, although shifted in wavenumber and with the off scale relative intensities. A better agreement between the theoretical and experimental results is possible if (a) the solvation is accounted for in the calculations and (b) a higher level of theory could be used.<sup>24</sup> In this context, the  $\nu_{\text{O–H}}$  signal at  $3402\text{ cm}^{-1}$  can be ascribed to intramolecularly hydrogen-bonded O–H groups in **1<sub>a</sub>**. The  $\nu_{\text{O–H}}$  vibrations at  $3581$  and  $3460\text{ cm}^{-1}$  are in fact a composite of three O–H vibrations

- (21) (a) Osawa, E.; Musso, H. *Angew. Chem., Int. Ed. Engl.* **1983**, *22*, 1. (b) Halgren, T. A. *J. Am. Chem. Soc.* **1992**, *114*, 7827–7843. (c) Halgren, T. A. *J. Comput. Chem.* **1996**, *17*, 616–641.  
 (22) (a) Gellman, S. H.; Dado, G. P. *Tetrahedron Lett.* **1991**, *50*, 7377–7380. (b) McDonald, D. Q.; Still, W. C. *Tetrahedron Lett.* **1992**, *33*, 7743–7747. (c) Dado G. P.; Gellman, S. H. *J. Am. Chem. Soc.* **1994**, *116*, 1054–1062.  
 (23) Stewart, J. J. P. *Semiempirical Molecular Orbital Methods. In Reviews in Computational Chemistry*; Lipkowitz, K. B., Boyd, D. B., Eds.; VCH: New York, 1990; Vol. 1, p 45.  
 (24) We have attempted, but unsuccessfully due to the molecular size, to implement higher level calculations in a reasonable amount of time.

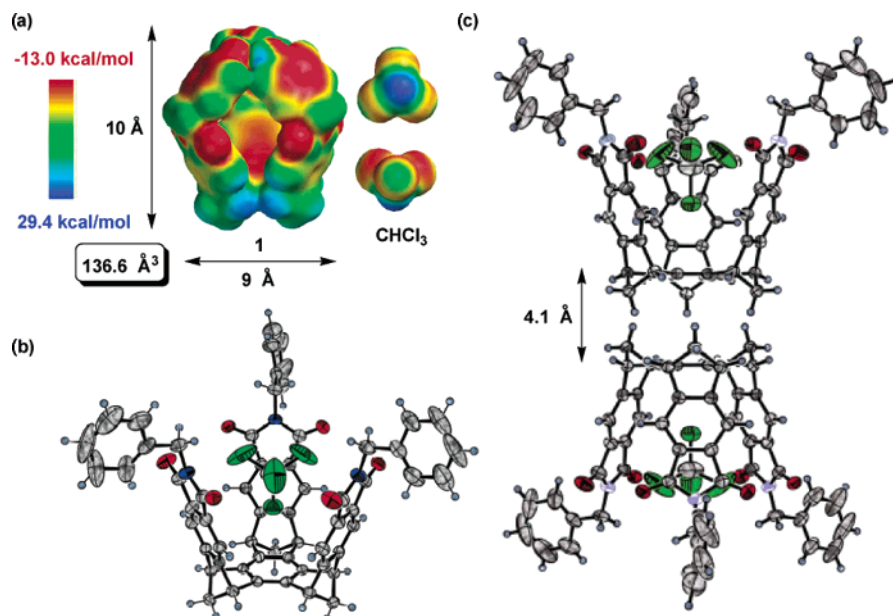


**Figure 7.** (a) Electrostatic potential surface map of **1** and  $\text{CHCl}_3$ , calculated using the AM1 method within Spartan Software. (b) ORTEP representation of the structure of the  $2 \cdot \text{CHCl}_3$  complex in the solid state. (c) A  $\pi$ - $\pi$  stacked dimer of **2**.

and correspond to three hydroxyl groups in **1<sub>b</sub>**. Comparing the experimental and simulated IR spectra, it is likely that the conformers **1<sub>b-a</sub>** contribute more significantly to the equilibrium. As the conformer **1<sub>a</sub>** that encloses space dominates the equilibrium, the designed receptor could operate as intended. We are, however, already examining various possibilities to completely bias the conformational balance toward **1<sub>a</sub>**.

**Acid/Base Titrations.** One of the reasons for studying gated molecular receptors such as **1–3** is to develop molecular devices that can be acid/base driven. We were therefore motivated to subject **1** to deprotonation and subsequent reprotonation conditions and demonstrate a reversible cycle. The chemical shifts for  $\text{H}_g$  and  $\text{H}_h$  protons, in the  $^1\text{H}$  NMR spectrum of **1** are affected by addition of triethylamine and practically restored by subsequent addition of trifluoroacetic acid, Figure 6. Specifically, addition of  $\text{Et}_3\text{N}$  to a  $\text{CDCl}_3$  solution of **1** resulted in a change in its  $^1\text{H}$  NMR spectrum, Figure 6. The resonance for  $\text{H}_g$  was shifted upfield from  $\delta = 7.04$  to 6.96 ppm, whereas the resonance for  $\text{H}_h$  changed from  $\delta = 6.64$  to 6.56 ppm. Interestingly, the resonances for other protons stayed unaffected. A 9-fold excess of  $\text{Et}_3\text{N}$  is evidently required to fully complex all three phenol units in **1**. It is therefore likely that hydrogen bonding interaction [ $\text{Et}_3\text{N} \cdots \text{H}-\text{OAr}$ ] rather than proton transfer dominates in our system. This is further vindicated by the fact that for the proton transfer to occur in related aliphatic amine/phenol complexes, sufficiently acidic phenols in more polar solvents are required.<sup>25</sup> The completely screened O–H groups in the complexed **1** are incapable of interacting intramolecularly, and the receptor gates are therefore prevented from forming a cyclic array of hydrogen bonds as shown in **1<sub>a</sub>**. Subsequent addition of a strong acid  $\text{CF}_3\text{CO}_2\text{H}$  practically restored the chemical shifts for  $\text{H}_h$  and  $\text{H}_g$  in the  $^1\text{H}$  NMR spectrum of **1**,

supporting the contention that an acid/base input can be used to reversibly affect the conformational equilibrium in **1** and related molecules.

**Recognition Studies.** The egg-shaped cavity of **1** is  $136.6 \text{ \AA}^3$  in volume and approximately  $10 \text{ \AA}$  tall and  $9 \text{ \AA}$  wide, Figure 7.<sup>26</sup> The interior of the cavity has walls built of electron-deficient phthalimides. Interestingly, the electrostatic potential map of the concave interior surface of **1** appears to have negative electrostatic potentials, suggesting electron-deficient molecules could be bound as potential guests, Figure 7a.<sup>27</sup> The outer convex surface is, in contrast, electron-deficient. A chloroform molecule is  $74.9 \text{ \AA}^3$  in volume,<sup>26</sup> with both shape and electrostatic potential that are complementary to the receptor's interior. If trapped inside of **1**, chloroform would occupy 54.8% of its interior volume, which is proportionate to the packing coefficient of liquids and is a good sign for molecular recognition in the liquid state.<sup>26</sup> We have attempted to observe the encapsulation of various guests including chloroform, at ambient and lower temperatures, in  $\text{CDCl}_3$  and  $\text{CD}_2\text{Cl}_2$ , using  $^1\text{H}$  NMR spectroscopy. The highly dynamic nature of **1**, in combination with its limited solubility in solvents which are not capable of occupying the interior of the cavity, prevented us from observing and studying the guest exchange in solution. Further studies are being conducted in our laboratory wherein the fine balance between the dynamic nature of these newly designed receptors and thermodynamics of the molecular encapsulation are under examination. A single-crystal X-ray study of **2**, however, revealed a disordered chloroform molecule positioned inside the cavitand along its  $C_3$  axis, as shown in Figure 7b.<sup>28</sup> The three nonfunctionalized aromatic gates are situated on the opposite side of the cavity and arranged in a propeller fashion. The unit cell is comprised of dimers of **2**, organized along the crystallographic  $c$ -axis, facing each other using base trisubstituted benzenes at a  $4.1 \text{ \AA}$  distance, indicating weak

(25) (a) Taft, R. W.; Gurka, D.; Joris, L.; Schleyer, P. Von R.; Rakshys, J. W. *J. Am. Chem. Soc.* **1969**, *91*, 4801–4808. (b) Hudson, R. A.; Scott, R. M.; Vinogradov, S. N. *J. Phys. Chem.* **1972**, *76*, 1989–1993. (c) Ilczyszyn, M.; Ratajczak, H. *J. Mol. Liq.* **1995**, *67*, 125–131. (d) Menger, F. M.; Barthelemy, P. A. *J. Org. Chem.* **1996**, *61*, 2207–2209. (e) Hannon, C. L.; Bell, D. A.; Kelly-Rowley, A. M.; Cabbel, L. A.; Anslyn, E. V. *J. Phys. Org. Chem.* **1997**, *10*, 396–404.

(26) The inner volume of **1** was calculated following Rebek's protocol. See: Mecossi, S.; Rebek, J., Jr. *Chem.—Eur. J.* **1998**, *4*, 1016–1022.

(27) Kamieth, M.; Klämer, F.-G.; Diederich, F. *Angew. Chem., Int. Ed.* **1998**, *37*, 3303–3306.

$\pi$ - $\pi$  aromatic attraction, Figure 7c. The observed stacking geometry is generally not preferred in aromatic interactions.<sup>32</sup> In the crystal structures of other tris-bicycloannelated benzenes C-H/ $\pi$  interactions are usually seen.<sup>33</sup> We reason that herein observed stacking could be ascribed to the following: (1) reduced aromaticity of the central benzenes due to their bond alternation and distortion imposed by bicyclic annelation<sup>34</sup> and

(2) tendency for a high packing coefficient in the crystal<sup>35</sup> that is attained by interdigitation of the CH<sub>2</sub> bicyclic bridges.

## Conclusions

The research described in this paper is projected toward developing multivalent molecular receptors that may potentially operate in a stimuli-responsive fashion to regulate molecular encapsulation, i.e., guest transport in/out of the host. As a first step toward that goal, we developed the synthesis of dynamic molecular containers having a set of functionalized aromatic rings installed at the rim to assemble on top of the cavitand via hydrogen bonding. Indeed, experimental and theoretical studies have, in unison, demonstrated that these compounds have a tendency to associate intramolecularly and prefer a conformation whereby all three aromatic rings are involved in a cyclic array of intramolecular hydrogen bonding, thus forming a fully closed receptor. The recognition properties have been preliminarily examined and have evidenced the dynamic nature of the receptor and its propensity toward hosting small guest molecules. Studies in our laboratory are now focused on the next challenge, which is to understand the operation of this and related molecular devices in controlling the encapsulation of guests.

**Acknowledgment.** Financial support of this research was supported by the Ohio State University. Generous computational resources were provided by the Ohio Supercomputer Center.

**Supporting Information Available:** Detailed descriptions of experimental methods, synthetic procedures, calculations, and X-ray crystallographic data for **2**. Complete list of authors for ref 19b. This material is available free of charge via the Internet at <http://pubs.acs.org>.

JA060534L

- (28) Crystal data for **2**·CHCl<sub>3</sub>: C<sub>60</sub>H<sub>39</sub>N<sub>3</sub>O<sub>6</sub> + CHCl<sub>3</sub>, formula weight = 1017.31, trigonal, space group *R*3̄, colorless plate, *a* = 16.326(1) Å, *c* = 32.400(4) Å, *T* = 150 K, *Z* = 6, *R*1(*F*) = 0.118, and *wR*2(*F*<sup>2</sup>) = 0.298 on all the data. The structure was solved by the direct methods procedure in SHELXS-97.<sup>29</sup> Molecule **2** contains a crystallographic three-fold rotation axis. There is a molecule of CHCl<sub>3</sub> disordered on this three-fold axis, with one chlorine atom and the carbon atom located on this axis and the remaining two chlorine atoms and one hydrogen atom disordered over the three sites related by the three-fold rotation. There is another region of disorder which is located outside of the cavity of the main molecule, and it is not within bonding range of it. Because the identity of the molecule in this region cannot be determined, it is modeled as three carbon atoms, C(1A), C(2A), and C(3A), with each assigned an occupancy factor of 0.5. Full-matrix least-squares refinements based on *F*<sup>2</sup> were performed in SHELXL-97,<sup>30</sup> as incorporated in the WinGX package.<sup>31</sup> The hydrogen atoms were added to molecule **2** at calculated positions using a riding model with *U*(H) = 1.2\**U*<sub>eq</sub> (attached atom). The final refinement cycle was based on 2939 intensities and 235 variables. The three largest peaks in the final difference map, ranging from 1.43 to 0.93 e/Å<sup>3</sup>, are in the immediate vicinity of the disordered CHCl<sub>3</sub> molecule. The next three largest peaks, ranging from 0.79 to 0.65 e/Å<sup>3</sup>, are located in the region of the disordered "solvent" atoms of C(1A), C(2A), and C(3A). It may be possible that these large final *R* factors are the result of insufficient modeling of the disordered CHCl<sub>3</sub> and "solvent" molecules.
- (29) Sheldrick, G. M. *SHELXS-97*; Universitat Göttingen: Göttingen, Germany, 1997.
- (30) Sheldrick, G. M. *SHELXL-97*; Universitat Göttingen: Göttingen, Germany, 1997.
- (31) Farrugia, L. J. *J. Appl. Crystallogr.* **1999**, *32*, 837–838.
- (32) (a) Hunter, C. A.; Sanders, J. K. M. *J. Am. Chem. Soc.* **1990**, *112*, 5525–5534. (b) Hunter, C. A.; Lawson, K. R.; Perkins, J.; Urch, C. J. *J. Chem. Soc., Perkin Trans.* **2001**, *2*, 651–669. (c) Keyser, E. A.; Castellano, R. K.; Diederich, F. *Angew. Chem., Int. Ed.* **2003**, *42*, 1210–1250.
- (33) Frank, N. L.; Baldrige, K. K.; Gantzel, P.; Siegel, J. S. *Tetrahedron Lett.* **1995**, *36*, 4389–4392 and references therein.
- (34) (a) Siegel, J. *Angew. Chem., Int. Ed. Engl.* **1994**, *33*, 1721–1723. (b) Buergi, H.-B.; Baldrige, K. K.; Hardcastle, K.; Frank, N. L.; Gantzel, P.; Siegel, J. S.; Ziller, J. *Angew. Chem., Int. Ed. Engl.* **1995**, *34*, 1454–1456.

- (35) Kitaigorodsky, A. I. *Molecular Crystals and Molecules*; Academic Press: New York, 1973.